

Curvature Preserving Fingerprint Ridge Orientation Smoothing using Legendre Polynomials

Surinder Ram, Horst Bischof
Graz University of Technology, Institute for Computer Graphics and Vision
{ram, bischof}@icg.tugraz.at

Josef Birchbauer
Siemens Austria
Siemens IT Solutions and Services, Biometrics Center
josef-alois.birchbauer@siemens.com

Abstract

Smoothing fingerprint ridge orientation involves a principal discrepancy. Too little smoothing can result in noisy orientation fields (OF), too much smoothing will harm high curvature areas, especially singular points (SP). In this paper we present a fingerprint ridge orientation model based on Legendre polynomials. The motivation for the proposed method can be found by analysing the almost exclusively used method in literature for orientation smoothing, proposed by Witkin and Kass [5] more than two decades ago. The main contribution of this paper argues that the vectorial data (sine and cosine data) should be smoothed in a coupled way and the approximation error should not be evaluated employing vectorial data. For evaluating the proposed method we use a Poincaré-Index based SP detection algorithm. The experiments show, that in comparison to competing methods the proposed method has improved orientation smoothing capabilities, especially in high curvature areas.

1. Introduction

Fingerprint-based authentication is one of the most widely applied biometric modalities. The existence of a large number of commercial fingerprint verification systems emphasizes the effectiveness of this type of biometrics. Fingerprints are attractive for identification because they can characterize a person uniquely and their configuration does not change through the life of individuals.

As described in [4], three types of characteristic features can be extracted from a Fingerprint image: a) patterns, which are the macro details of a fingerprint such as ridge flow and pattern type. b) minutiae, which are points where

ridges bifurcate or end. c) pores, edge contours, incipient ridges, breaks, creases and other permanent details.

While the third mentioned feature type, such as pores, are difficult to apply in an Automatic Identification System (AFIS), minutiae represent the back end of these systems. Additionally, fingerprint patterns are used to assist the matching procedure. Automatic fingerprint recognition requires that the input image is matched with a large number of fingerprints stored in a database. Using flow patterns one can categorize a fingerprint into a number of classes. The need for this classification results from the fact that large volumes of fingerprints can be partitioned into smaller subsets and thus a search can be made faster.

Despite decades of research, fingerprint matching is still considered to be a difficult problem, mainly due to the large variability in different impressions of the same finger (i.e. displacement, rotation, distortion, noise, etc.). One way to relax the problem in terms of performance and runtime is to use certain 'landmarks' in the image in order to align two fingerprints on each other. Such landmarks can be extracted from fingerprint patterns in form of singular points (SPs). SPs occur at positions where the ridge flow is discontinues. Usually, these points can be categorized into core and delta type singularities.

Ridge orientation is inevitably used for detecting, describing and matching fingerprint features such as minutiae and SPs. Large efforts are made in order to extract reliable orientation data from fingerprints. Many methods for ridge orientation estimation exist in the literature [1]. Unfortunately, determination of ridge orientation becomes more difficult when image quality is low. Thus even the 'best' orientation estimation algorithm will fail in regions of low image quality. To encounter this problem, the ridge orientation is smoothed. It is noteworthy to mention, that only small regions can be smoothed successfully.

The almost exclusively used method in literature as well as in commercial fingerprint matching modules for smoothing orientation has been brought up by Witkin and Kass [5] more than 20 years ago. Their paper describes a solution for the problem of discontinuities which occur at angles of 180 and 0 degrees. In this paper we explain one of the limiting problems of this method, namely smoothing high curvature areas. Furthermore, we discuss why this issue limits the orientation smoothing capability of numerically averaging methods as well as of the more sophisticated mathematical fingerprint ridge orientation models. We present a model based method which allows higher smoothing levels without degrading the existing orientation information in high curvature areas. The rest of the paper is organised as described in the following. In Section 2 we discuss related work. Section 3 summarises the problem of ridge orientation smoothing in high curvature areas and the resulting trade offs. In Section 4 our proposed method is described. Experiments, showing the ridge orientation smoothing capability of the proposed method are given in Section 5. Finally, the summary of this paper can be found in Section 6.

2. Related Work

In digital images, the gradients direction can be extracted for the full 360 degree range. Ridge orientation, which is orthogonal to these image gradients, can be determined only up to 180 degrees. Smoothing orientation is not straightforward. Orientation vectors cannot be averaged in their local neighbourhood since opposite orientation vectors would cancel each other, even if they correspond to the same orientation. This is caused by the fact that local orientations remain unchanged when rotated for 180 degrees. Witkin and Kass [5] proposed the doubling of the orientation angle (sometimes also denoted as squaring the orientation vector, see [1]). After doubling the angles, opposite gradient vectors will point in the same direction and therefore will reinforce each other, while perpendicular gradients will cancel. This procedure guarantees an continuous occurrence of sine and cosine data and thus enables standard filtering procedures (e.g. low pass filter) to be applied on orientation data. After averaging, the gradient vectors have to be converted back to their single angle representation. All currently available fingerprint ridge orientation models proceed by fitting vectorially models to the doubled angle orientation data.

A combination method is described by Zhou and Gu in [16, 15]. This method first describes the global orientation field using power series and than locally models singularities. Unfortunately, the algorithm is difficult to apply in practice, since combining the two parts of the model is cumbersome. The latter is especially true for noisy input images, which is the main motivation for modelling ridge orientation. Furthermore, the algorithm requires re-

liable detection of SPs. In [7], Li et al. model the orientation of fingerprints using higher order phase portraits. Therefore, the method divides the fingerprint into several predefined regions and approximates them using piecewise linear phase portraits. In a further step this method computes a global model using the piecewise linear phase portraits. Similar problems as describe above apply also to this algorithm, namely the required separation of fingerprints into predefined regions and the robust detection of SPs.

Recently Wang et al. [14] presented a Fingerprint Orientation Model based on trigonometric polynomials. Their approach (named FOMFE) does not require prior knowledge of SPs. The application includes orientation interpolation, SP detection and database indexing based on the model parameters. One of the authors claims, namely detection of SPs in low quality fingerprints, has not been tested using manually labelled data.

3. A survey of the smoothing problem

Every orientation smoothing approach which is based on the above mentioned approach of Witkin and Kass [5], will have a poor smoothing capability in high curvature areas. (see Figure 1 for an example). An explanation for the occurrence of this smoothing problem is given in Figure 2, where the vectorial orientation data of a loop type fingerprint is given. In the centre, these two surfaces contain a discontinuity, a jump from -1 to 1. The presence of this discontinuity is important, because the SP is defined by the root of this discontinuity. This fact can be easily verified by back conversion of the vectorial data using the formula $O = \frac{1}{2}(\arctan \frac{\sin(2O)}{\cos(2O)})$. Smoothing the vectorial data results in shifting the roots of the sine and cosine data and hence in shifting of the SP. Furthermore, smoothing the discontinuity results in false orientation around the SP (see Figure 1). This problem plaques not only standard numerical methods but also every potential ridge orientation modelling approach. It is not important to precisely approximate the individual discontinuities. The reason therefore is that the appearance of a SP is strictly defined by the roots and the ratio of the two shown surfaces. Existing approaches put high emphasize on the exact and separate approximation of the vectorial data. In this paper, we show that the approximation should be done in a coupled way and that the above mentioned roots can be shifted back to the correct position, which leads to precise modelling of SPs.

4. Fingerprint Ridge Orientation Modelling using Legendre Polynomials

For ridge orientation estimation, we adapt a gradient based approach (Rao and Schunk [13]). The OF extraction is done pixel wise and is not averaged using any numerical

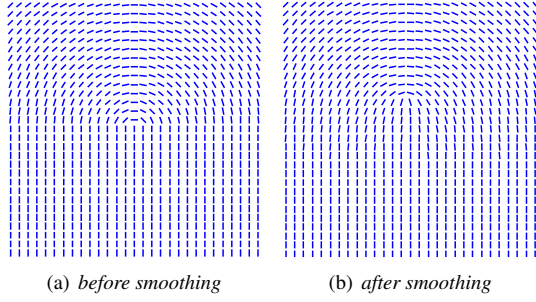


Figure 1. In **1(a)** the orientation field of a loop type fingerprint image can be seen. This image has been synthetically generated. In **1(b)** the orientation field after vectorial smoothing (using the approach of Witkin and Kass [5]) can be seen. The image size is 30x30 pixels. Smoothing is done using a 9x9 averaging filter. Note how the SP is shifted away from the low curvature area.

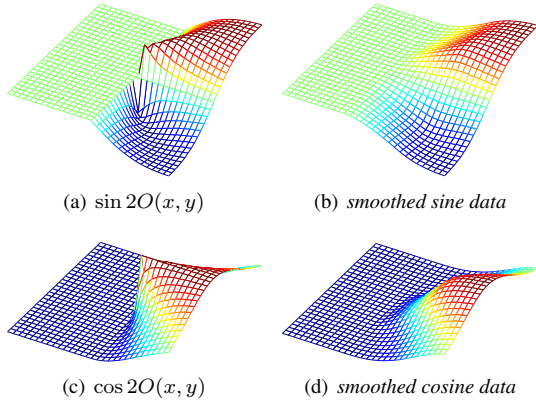


Figure 2. In **2(a)** and **2(c)** the vectorial data of a loop type fingerprint can be seen (as shown in Figure 1). In **2(b)** and **2(d)** these surfaces have been smoothed using an averaging filter of 9x9 pixels. An explanation why the SP shifts after smoothing can be given by looking at the cosine data. The root of the surface, which defines the position of the SP, has been shifted.

method. In the following, the doubled orientation is denoted with $2O(x, y)$.

4.1. Weighted Pseudoinverse Technique for Least Squares Approximation

For the approximation of a discrete two dimensional function $f(x, y)$ we propose to use a linear combination of n basis functions. Then for every point $\mathbf{x}_i = (x_i, y_i)$ the following equation can be evaluated:

$$f(x, y) \approx \sum_{j=0}^n a_j \phi_j(x, y) \quad (1)$$

Let

$$\Phi(\mathbf{x}_i) = [\phi_0(\mathbf{x}) \quad \phi_1(\mathbf{x}) \quad \dots \quad \phi_n(\mathbf{x})] \quad (2)$$

be the row vector containing the set of basis functions $[\phi_0(\mathbf{x}) \quad \phi_1(\mathbf{x}) \quad \dots \quad \phi_n(\mathbf{x})]$ evaluated for a given coordinate $\mathbf{x} = (x, y)$. Using this expression, we can define the system matrix \mathbf{V} :

$$\mathbf{V} = \begin{pmatrix} \Phi(\mathbf{x}_1) \\ \Phi(\mathbf{x}_2) \\ \vdots \\ \Phi(\mathbf{x}_i) \end{pmatrix} = \begin{pmatrix} \phi_0(\mathbf{x}_1) & \phi_1(\mathbf{x}_1) & \dots & \phi_n(\mathbf{x}_1) \\ \phi_0(\mathbf{x}_2) & \phi_1(\mathbf{x}_2) & \dots & \phi_n(\mathbf{x}_2) \\ \vdots & \vdots & \ddots & \vdots \\ \phi_0(\mathbf{x}_i) & \phi_1(\mathbf{x}_i) & \dots & \phi_n(\mathbf{x}_i) \end{pmatrix} \quad (3)$$

Where the size of the system matrix \mathbf{V} is determined by the number of coordinate points i and the number of basis functions n . Further, we can give the parameter vector as:

$$\mathbf{a} = [a_1, a_2, \dots, a_n]^T \quad (4)$$

and the vector of function values \mathbf{f} as:

$$\mathbf{f} = [f(\mathbf{x}_1), f(\mathbf{x}_2), \dots, f(\mathbf{x}_i)]^T \quad (5)$$

Where $f(\mathbf{x}_k)$ is the observed function value at the coordinate $\mathbf{x}_k = (x_k, y_k)$. We use the method of least squares to model the numerical data \mathbf{f} . The best fit is characterized by the least value of the sum of squared residuals \mathcal{F} . Furthermore, a weight ω to every pixel $\mathbf{x} = (x, y)$ is assigned because not all points are of equal value in determining a solution. Using this convention, we can write:

$$\mathcal{F} = \sum_{j=1}^i \omega_j [\Phi(\mathbf{x}_j) \mathbf{a}^T - f(\mathbf{x}_j)]^2. \quad (6)$$

Since the number of data points (and thus equations) is much larger than the number of basis functions, we use the pseudoinverse technique to estimate a solution [3, 11]:

$$\mathbf{a} = (\mathbf{V}^T \mathbf{W} \mathbf{V})^{-1} \mathbf{V}^T \mathbf{W} \mathbf{f} \quad (7)$$

Where $\mathbf{W} = \text{diag}(\omega_1, \dots, \omega_i)$ is the diagonal weighting matrix containing the weights for every coordinate.

4.2. Generating Basis Functions

Common polynomials are not suitable as basis functions because they result in a bad conditioned system of linear equations. We use Legendre polynomials as basis functions in our paper. These polynomials are orthogonal in the interval $[-1, 1]$, fast to evaluate and simple to generate. Another important advantage in behalf of orthogonal basis functions is that they span an Euclidean parameter space.

Each univariate Legendre polynomial $P_n(x)$, can be computed using Rodrigues formula [3]:

$$\phi_n(x) = \frac{1}{2^n n!} \frac{d^n}{dx^n} [(x^2 - 1)^n] \quad (8)$$

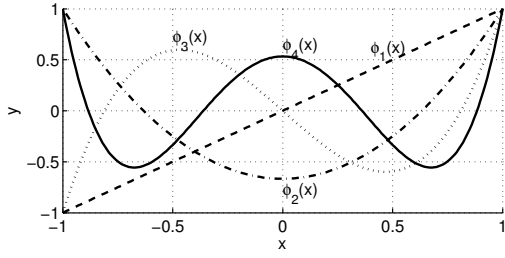


Figure 3. Function plot of some Legendre polynomial basis functions as given in Equation 9.

Figure 4.2 shows a few computed basis functions (given in Equation 9).

$$\begin{aligned}
 \phi_0(x) &= 1 & \phi_1(x) &= x \\
 \phi_2(x) &= \frac{3x^2 - 1}{2} & \phi_3(x) &= \frac{5x^3 - 3x}{2} \\
 \phi_4(x) &= \frac{35x^4 - 30x^2 + 3}{8} & \phi_5(x) &= \frac{63x^5 - 70x^3 + 15x}{8}
 \end{aligned} \tag{9}$$

Generalization to two dimensions can be done using the method of separable variables. Consider the Legendre polynomials $\phi_{n-m}(x)$ and $\phi_m(y)$ in the two variables x and y . Then one can compute the set of basis functions for the k^{th} order Legendre polynomial expansion as:

$$\phi_{nm} = \phi_{n-m}(x)\phi_m(y) \quad \left(\begin{array}{l} n = 0, 1, 2, \dots, k \\ m = 0, 1, 2, \dots, n \end{array} \right)$$

4.3. Optimization

The optimization for obtaining the final parameters for the vectorial data is done in two steps. In a first optimization step we roughly approximate the models parameters using the closed form solution described in Subsection 4.1. In a second step, a non-linear refinement delivers the accurate parameters. Our approach is not depending on other, prior computed data such as SPs.

Let \mathbf{a} and \mathbf{b} be the parameters of a Legendre expansion of the sine and cosine data respectively. Then, the orientation field can be computed as described in the following:

$$O(\mathbf{x}_j) = \frac{1}{2} \arctan \frac{\Phi(\mathbf{x}_j)\mathbf{a}^T}{\Phi(\mathbf{x}_j)\mathbf{b}^T} \tag{10}$$

From Equation 10 one can observe that \mathbf{a} and \mathbf{b} are coupled and influence the orientation in a non-linear way. Thus, the set of parameters cannot be computed independently from each other. Furthermore, the amplitude of each polynomial can be cancelled by the division - thus making smaller amplitudes more sensitive to noise and approximation errors. Moreover, the highly non-linear arctan function further propagates a possible error. The real measure for fitting

a ridge orientation model to a fingerprints orientation should be directly computed by using the orientation angle as opposed to its sine or cosine. This optimization can only be carried out using a non-linear technique. On the other hand, a single non-linear optimization would consume too much time for optimization. Furthermore, such a method needs a special treatment for local minima. This is the reason why we propose a hybrid optimization method which delivers accurate parameters and is still reasonable fast.

In order to minimize the least square error, the following non-linear function must be minimized:

$$\min_{\mathbf{a}, \mathbf{b}} \sum_{j=1}^i \omega_i \left[\arctan \frac{\Phi(\mathbf{x}_j)\mathbf{a}^T}{\Phi(\mathbf{x}_j)\mathbf{b}^T} - 2O(\mathbf{x}_j) \right]^2 \tag{11}$$

Where \mathbf{a} and \mathbf{b} are the desired parameter vectors for the Legendre approximation. The coordinates are being \mathbf{x}_j , the weight ω_i and i the number of points. As already discussed, handling orientation data needs special attention. In an early paper Rao and R. Jain [12] proposed the sine as a distance measure for non-linear parameter estimation in linear phase portraits. In their optimization routine, they minimize the absolute values of this measure. Later, Ford and Strickland [2] suggested that the sum of squares of these distances should be minimized. One should note that in these references the authors intention is to use directly the orientation to obtain the models parameters. As we carry out our optimization already in the doubled angle space, we have to half the angle for correct determination of the error functional. Then, rewriting the cost function results in:

$$\min_{\mathbf{a}, \mathbf{b}} \sum_{j=1}^i \omega_i \left[\sin \left(\frac{1}{2} \arctan \frac{\Phi(\mathbf{x}_j)\mathbf{a}^T}{\Phi(\mathbf{x}_j)\mathbf{b}^T} - O(\mathbf{x}_j) \right) \right]^2 \tag{12}$$

4.3.1 First Step

In the first optimization step, we propose to independently model the sine and cosine data of the given orientation field $O(x, y)$. The parameter estimation proceeds as described in Subsection 4.1. Therefore it is necessary to compute the weighted pseudo inverse of the system matrix $\mathbf{V}_w^+ = (\mathbf{V}^T \mathbf{W} \mathbf{V})^{-1} \mathbf{V}^T$. Note that the coordinates x and y need to be normalised to the range $[-1, 1]$. The system matrix \mathbf{V} is only depending on the x and y coordinates and can be precomputed for a given image size. The weighting matrix \mathbf{W} is computed using fingerprint segmentation, $\omega = 0$ for background and $\omega = 1$ for foreground pixels. The parameter vector \mathbf{a} and \mathbf{b} for the sine and cosine approximation can be computed as described in the following:

$$\begin{aligned}
 \mathbf{a}_0 &= \mathbf{V}_w^+ \mathbf{W} \mathbf{f}_1 \\
 \mathbf{b}_0 &= \mathbf{V}_w^+ \mathbf{W} \mathbf{f}_2
 \end{aligned} \tag{13}$$

\mathbf{f}_1 and \mathbf{f}_2 contain the sine and cosine data.

$$\begin{aligned}\mathbf{f}_1 &= [\sin 2O(\mathbf{x}_1), \sin 2O(\mathbf{x}_2), \dots, \sin 2O(\mathbf{x}_i)]^T \\ \mathbf{f}_2 &= [\cos 2O(\mathbf{x}_1), \cos 2O(\mathbf{x}_2), \dots, \cos 2O(\mathbf{x}_i)]^T\end{aligned}$$

4.3.2 Second Step

The cost function in Equation 12 is minimized in a simple non-linear optimization algorithms. Therefore, a line search based algorithm proceeds by computing a search direction d_{iter} followed by the decision how far to move along that directions.

$$\mathbf{c}_{iter+1} = \mathbf{c}_{iter} + \alpha_{iter}d_{iter} \quad (14)$$

Where \mathbf{c} consists of the concatenated parameter vectors $\mathbf{c} = [\mathbf{a}, \mathbf{b}]$ and α_{iter} is the estimated search step size. We use numerical evaluations of the cost function in order to compute the derivatives which are necessary to compute the search direction α_{iter} . The iterative, quasi-newton based approach always tries the step length $d_{iter} = 1$ and will accept this value if the Wolfe conditions [10] are satisfied.

The initial parameters \mathbf{a}_0 and \mathbf{b}_0 are computed using the closed form solution and provide a good starting position. Therefore the maximum number of iterations is set to 100. If the minima is detected before the maximum number of iterations has been exceeded, the algorithms quits and returns the current parameters. This process uses typically 5 seconds (3 to 10 seconds, depending on the image) on a state of the art computer (Intel Core Duo 2.4 GHz, Matlab 7.2) for typical image sizes of 388x374. It should be mentioned that the computation could be carried out much faster using more sophisticated optimization methods. Furthermore, using a lower resolution OF can massively speed up the computation process.

5. Evaluation

For evaluation of the ridge orientation model, we conduct SP detection on a publicly available database. Note, that here the task of singular point detection is used as a benchmark for evaluating the quality of the proposed ridge orientation model. This becomes evident as all existing SP detection algorithms depend on a correctly estimated OF, including robust methods (eg. [9]) which tolerate noise to some extent. Algorithms for SP detection are described in [4, 1, 9].

The used database (FVC2004 DB3A [8], 800 images) includes images of low quality, thus it represents a good subject for testing the ridge orientation smoothing ability. For the detection of SPs, we use the Poincaré-Index based approach described by Kawagoe and Tojo [6]. The method proceeds by numerical integration of the angle along a given curve. The performance of this method is affected by noise

in the orientation field. Thus it is suggested [1] to smooth the orientation field before detecting SPs. Naturally, this comes with a trade off. In particular, one has to make a compromise between missing singularities (false negatives due to excessive smoothing) or spurious singularities (false positives, occur due to too low smoothing). We use the Poincaré-Index computed over a 9x9 pixel rectangle for SP detection. All SPs in the 800 images have been manually labelled.

We compare three different OF smoothing approaches. The first method is smoothing the pixel wise extracted orientation data using Gaussian convolution (described in [1] by Bazen and Gerez). The second method is described in [14] by Wang et al. and proceeds by fitting two-dimensional Fourier series to the orientation field. Both methods base their smoothing feature on the doubled angle averaging method of Witkin and Kass [5]. For orientation smoothing using convolution, we employ a $\sigma = 5, 25$ and 12 (optimal value as of [1]). Ridge orientation modelling using Fourier-Series is done exactly as described in [14], the parameter k has been varied between $k = 2, 4$ and 6.

In Figure 4 the orientation smoothing capability of different methods is illustrated. Ridge orientation 4(b) has been extracted using a gradient based method from the original image 4(a). Subfigure 4(i), 4(h) and 4(g) show the orientation field smoothed using Gaussian convolution. While low smoothing ($\sigma = 5$ in 4(i)) causes wrong detections, too much smoothing ($\sigma = 25$ in 4(g)) usually causes a smoothing of the high curvature area and results in a poor overall orientation field. In Subfigure 4(d), 4(e) and 4(f) the orientation modelling capability of the FOMFE approach [14] is shown. In 4(d) we use a second order trigonometric polynomial with 50 parameters. The reconstructed orientation in the noise affected area is not satisfactory. In 4(e) the optimal number of 162 parameters is used and in 4(f) we used 338 parameters for describing the orientation. Note that in both cases wrong singularities are detected. In Subfigure 4(c) the computed orientation of our proposed method is shown. Emphasize should be paid on the correct reconstruction of the orientation in the noise affected region and to the accurate determination of the SPs position.

Figure 5 illustrates how the second optimization step proceeds. The fingerprint image is the same as shown in Figure 4(a) and the orientation has been estimated as shown in Figure 4(b). The first image 5(a) is derived from the closed form optimization formula. By further optimization using the described non-linear approach, SPs arise and move closer to their real position (seen in 5(b) and 5(c)). Furthermore, it can be seen how the global orientation field (especially in the noisy region) incrementally converges to the real one. After 17 iterations 5(d) the orientation approximation has already reached a satisfactory level. The final result after 100 iterations is given in Figure 4(c).

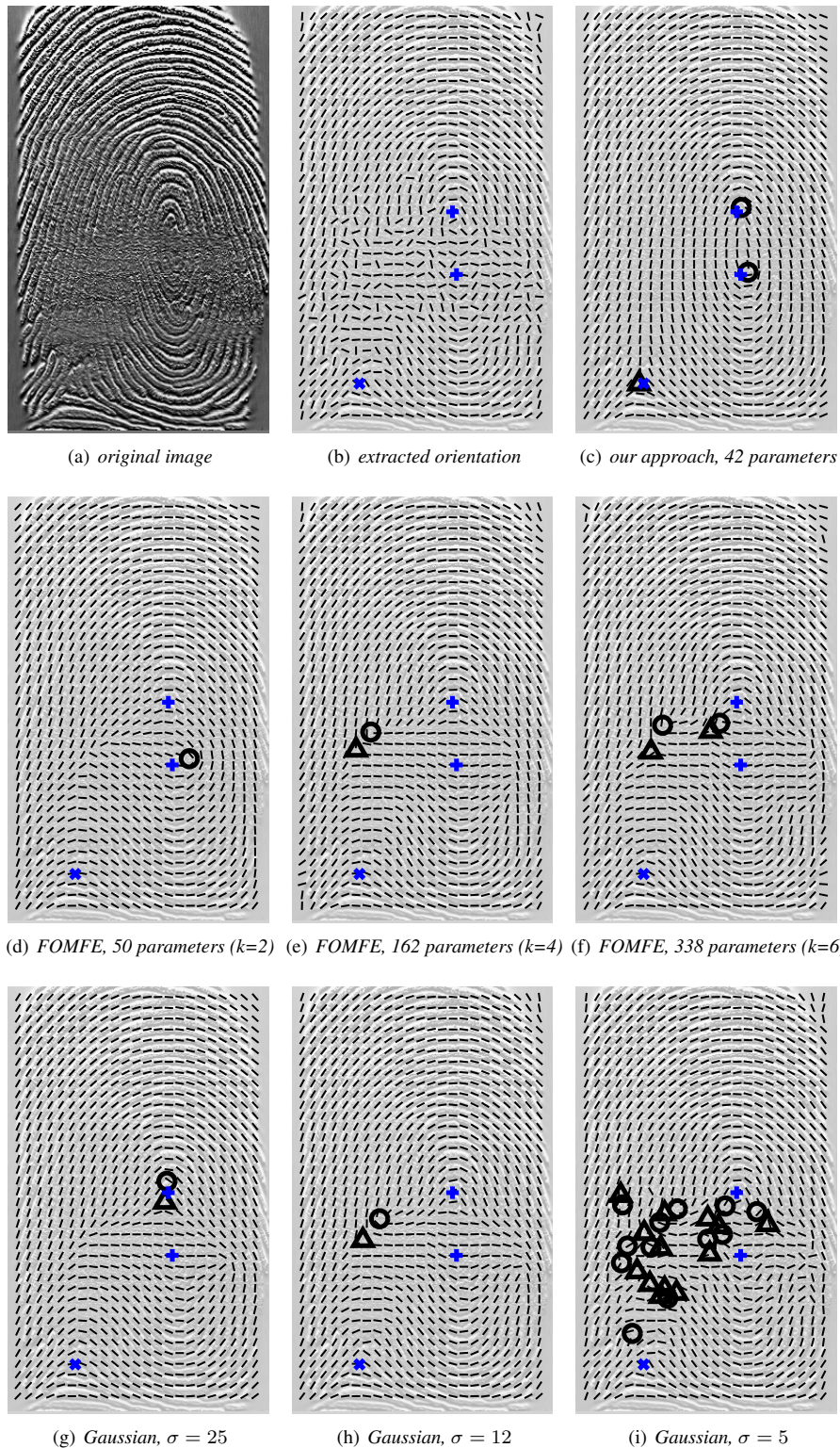


Figure 4. In 4(b) the orientation field of a partially noisy fingerprint image 4(a) can be seen. Manually labelled SPs are shown as '+' and 'x', detected cores as 'O' and deltas as 'Δ'. The second row shows ridge orientation smoothed using the FOMFE approach as described in [14]. The orientation model has been varied between heavy smoothing 4(d), optimal value 4(e) and low smoothing 4(f). A similar sequence has been created in the third row, where the smoothing is done using convolution with a Gaussian. In 4(c) the proposed method is shown. Both, the high curvature area as well as the global orientation field have been reconstructed more accurately in contrast to the other methods.

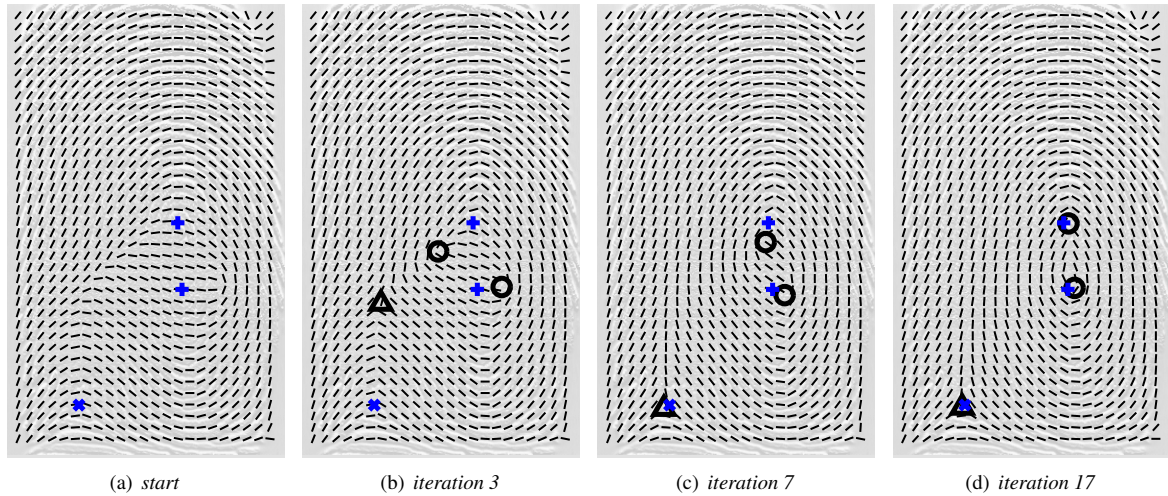


Figure 5. Illustration of the second optimization step (using the same input data as shown Figure 4). In 5(a) the output of the closed form optimization can be seen. In 5(b), 5(c) and 5(d) it is illustrated how the non-linear method converges towards the final solution, which is shown in Figure 4(c).

5.1. Performance Measures

For measuring the performance of an SP detection algorithm, the two quantities of interest are clearly the number of correct detections and the number of spurious detections. Obviously, the ultimate goal is to maximize the number of correct detections and to minimize wrong detections.

Unfortunately, there is no established 'standard' in literature for evaluating SP detection approaches. Although most authors give true positive and false positive numbers, there seems to be no consensus on how large the threshold should be, on which this decision is based on. In this publication, we intend to vary this threshold and display all figures as a function of it. The definition of the performance measures is given in the following:

$$\text{Recall} = \frac{TP}{TP + FN} \quad (15)$$

$$\text{Precision} = \frac{TP}{TP + FP} \quad (16)$$

$$\text{F-Measure} = \frac{2 \cdot \text{Recall} \cdot \text{Precision}}{\text{Recall} + \text{Precision}} \quad (17)$$

Where TP =true positive, FN =false negative and FP =false positive. The first quantity of interest, namely, the proportion of SPs that are detected, is given by the recall. The second quantity of interest is the number of correct detections relative to the total detections made by the system is given by the precision. As we are interested in which method achieves the best trade-off between these two quantities, we need a third measure. The F-Measure summarizes the trade-off between recall and precision, giving equal importance to both.

5.2. Experimental Results

Figure 6 shows the results for SP detection in the FVC2004 3a database. Low smoothing results in good recall figures. This is due to a) the fact that fewer SPs are 'missed' during the detection (because they were not smoothed out) and b) due to the fact that noisy OFs contain many random detections which may be counted as true positive. On the other hand, low smoothing results in poor precision rates. Both this findings can be observed in Figure 6(b) and 6(a) for the Gaussian smoothed orientation field ('Gaussian $\sigma = 5$ ') as well as for the FOMFE model ('FOMFE338'). In defence of FOMFE it should be mentioned that it performs much better on the precision figures as compared to Gaussian smoothing.

The other performed scenario is the heavy smoothing of orientation fields ('FOMFE50' and 'Gaussian $\sigma = 25$ '), Figure 6(a) and 6(b). Ideally, one would expect that more smoothing results in better precision figures and in worse recall figures. Unfortunately, this findings can not be observed in practice, since heavy smoothing shifts the position of the SPs beyond any usable thresholds. Therefore, heavy smoothing results in bad precision and bad recall numbers.

The trade off between the above mentioned two scenarios is denoted with 'FOMFE162' and 'Gaussian $\sigma = 12$ '. These values have been suggested by the corresponding authors [14, 1]. As can be seen in Figure 6, our approach scores very high precision and recall figures. The trade off, smoothing artefacts while preserving high curvature areas, has been significantly improved (F-Measure 10% increased) using the proposed method.

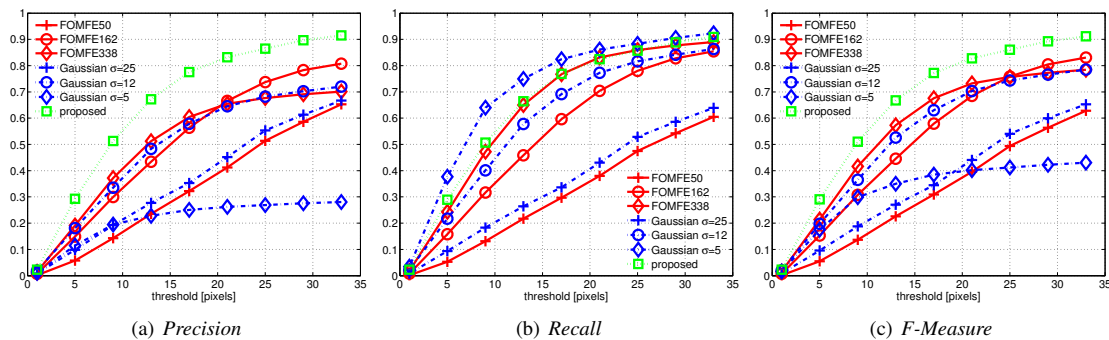


Figure 6. Recall, Precision and the F-Measure evaluated for different Fingerprint Ridge Orientation smoothing approaches using the FVC2004 3a [8] database. On the y-axis, the threshold for obtaining the mentioned performance measures is given.

6. Conclusion

In this paper we proposed a novel method for fingerprint ridge orientation modelling using Legendre Polynomials. The method proceeds in two steps. In the first optimization step we roughly estimate the parameters using a closed form solution. In the second optimization step, we propose to use a non-linear optimization technique for more precise parameter estimation. The motivation for the second step can be found by analysing the almost exclusively used method in literature for orientation smoothing, proposed by Witkin and Kass [5] more than 20 years ago. In the main contribution of this work, it is demonstrated that vectorial orientation data (sine and cosine data) should be smoothed simultaneously and that the approximation quality should be evaluated directly using the orientation angle. For evaluation of the proposed method we use a Poincaré-Index based SP detection algorithm. The experiments show, that the proposed method has improved orientation smoothing capabilities in comparison to other methods. Furthermore, the presented approach requires only a small number of parameters for global ridge orientation description.

Acknowledgments.

This work has been funded by the Biometrics Center of Siemens IT Solutions and Services, Siemens Austria.

References

- [1] A. M. Bazen and S. H. Gerez. Systematic methods for the computation of the directional fields and singular points of fingerprints. *PAMI*, 24(7):905–919, 2002. 1, 2, 5, 7
- [2] R. M. Ford and R. N. Strickland. Nonlinear models for representation, compression, and visualization of fluid flow images and velocimetry data. In *Visualization and Machine Vision, 1994. Proceedings., IEEE Workshop on*, pages 1–12, Seattle, WA, USA, 1994. IEEE Computer Society. 4
- [3] P. George. *Interpolation and Approximation by Polynomials*. Canadian Mathematical Society, 2003. 3
- [4] A. K. Jain and D. Maltoni. *Handbook of Fingerprint Recognition*. Springer-Verlag New York, Inc., Secaucus, NJ, USA, 2003. 1, 5
- [5] M. Kass and A. Witkin. Analyzing oriented patterns. *Comput. Vision Graph. Image Process.*, 37(3):362–385, 1987. 1, 2, 3, 5, 8
- [6] M. Kawagoe and A. Tojo. Fingerprint pattern classification. *Pattern Recogn.*, 17(3):295–303, 1984. 5
- [7] J. Li, W. Yau, and H. Wang. Constrained nonlinear models of fingerprint orientations with prediction. *PR*, 39(1):102–114, January 2006. 2
- [8] D. Maio, D. Maltoni, R. Cappelli, J. L. Wayman, and A. K. Jain. Fvc2004: Third fingerprint verification competition. In D. Zhang and A. K. Jain, editors, *ICBA*, volume 3072 of *Lecture Notes in Computer Science*, pages 1–7. Springer, 2004. 5, 8
- [9] K. Nilsson and J. Bigun. Localization of corresponding points in fingerprints by complex filtering. *Pattern Recogn. Lett.*, 24(13):2135–2144, September 2003. 5
- [10] J. Nocedal and S. J. Wright. *Numerical Optimization*. Springer, second edition, 2006. 5
- [11] R. Penrose. On best approximate solution of linear matrix equations. *Proceedings of the Cambridge Philosophical Society*, 52(52):17–19, 1956. 3
- [12] A. R. Rao and R. Jain. Analyzing oriented textures through phase portraits. *Pattern Recognition, 1990. Proceedings., 10th International Conference on*, i:336–340 vol.1, 1990. 4
- [13] A. R. Rao and B. G. Schunck. Computing oriented texture fields. *Computer Vision and Pattern Recognition, 1989. Proceedings CVPR '89., IEEE Computer Society Conference on*, pages 61–68, 1989. 2
- [14] Y. Wang, J. Hu, and D. Phillips. A fingerprint orientation model based on 2d fourier expansion (fomfe) and its application to singular-point detection and fingerprint indexing. *PAMI*, 29(4):573–585, April 2007. 2, 5, 6, 7
- [15] J. Zhou and J. Gu. A model-based method for the computation of fingerprints' orientation field. *IP*, 13(6):821–835, June 2004. 2
- [16] J. Zhou and J. Gu. Modeling orientation fields of fingerprints with rational complex functions. *PR*, 37(2):389–391, February 2004. 2